An Overview of Atomic Processes for Kilonovae

Nigel Badnell

Department of Physics
University of Strathclyde
Glasgow, UK

Overview

LTE $\lesssim 1$ week:

- Saha–Boltzmann fractional ionic abundances and level populations
  - 'Just' need opacities for the first few ionization stages of the lanthanides, actinides etc.

non-LTE $\gtrsim 1$ week:

- Fractional abundances need ionization and recombination rate coefficients
  - Compare dielectronic recombination (DR) vs radiative recombination (RR) rate coefficients for (tellurium) Te^{2+}
- Level population determination needs electron-impact excitation (EIE) rate coefficients and associated radiative rates
  - e.g. Distorted wave (DW) or R-matrix for EIE.

LTE

- Saha–Boltzmann fractional ionic abundances and level populations
- Need opacities for the first few ionization stages of the lanthanides, actinides etc.
- 'Expansion' vs 'line-binned' opacities
- Internal partition function

Lanthanide and Actinide Opacities

Kasen $et\ al$ (2013, 2017) have used AUTOSTRUCTURE (AS) to calculate data for all of the lanthanides for the first few charge states ($q = 0 - 4+$)

Tanaka $et\ al$ (2020) have used HULLAC similarly, while Banerjee $et\ al$ (2022) have extended the work to higher charge-states ($q = 10+$)

Fontes $et\ al$ (2020, 2023) have used CATS & RATS to calculate data for all of the lanthanides and actinides, for the first few charge states ($q = 0 - 3+$)

The Mons group has used GRASP/Cowan for a number of lanthanides for higher charge states ($q = 4 - 9+$) e.g. Carvajal Gallego $et\ al$ (2023).

UPDATES: Tanaka HULLAC+, Silva/Flors Optimized+calibrated FAC.
AS v30.x can generate the FAC potential internally and it is much faster/more memory efficient than FAC. (AS is potentially more flexible than FAC.)

Apart from U, actinide data is more limited, but likely necessary (Even $et\ al$ 2020) up to $Z = 98$, or so (Fontes $et\ al$ 2023).
UPDATE: Silva/Flors Optimized+calibrated FAC, work in progress.

Expansion Opacities

For a force-free uniform expanding medium, the monochromatic opacity (L^2/M) as a function of wavelngth, λ, as introduced by Kasen $et\ al$ (2013), is given by (Sobolev 1960, Karp $et\ al$ 1977, Eastman & Pinto 1993)

$$\kappa(\lambda) = \frac{1}{\rho c t_{\rm ej}} \sum_l \frac{\lambda_l}{\Delta\lambda} \left[1 - {\rm e}^{-\tau_l}\right] \tag{1}$$

where the lines (l) summed over lie within each wavelength bin $\Delta\lambda$, ρ is the material density, and $t_{\rm ej}$ the ejecta expansion time.

The optical depth (τ_l) of the line is given by

$$\tau_l = \pi\alpha \left(\frac{t_{\rm ej}}{\tau_0}\right) \left(\frac{\lambda_l}{a_0}\right) a_0^3 N_l f_l^{\rm abs} \tag{2}$$

in terms of the absorption oscillator strength $f_l^{\rm abs}$ for the line and the number density N_l of the lower level of the line.

This is referred to as the expansion opacity.

For $\tau_l \ll 1$

$$1 - \mathrm{e}^{-\tau_l} \approx \tau_l \tag{3}$$

which leads to the line-binned opacity form (Fontes $et\ al$ 2020, 2023).

The problem with Eq.(1) is that the atomic physics and the macroscopic physics are not de-coupled, complicating data archiving, see e.g. the Tanaka $et\ al$ (2020) tables as a function of density, temperature, electron fraction.

The advantage of using (3) is that the atomic physics and the macroscopic physics are de-coupled. Opacity data can be archived independently.

Compact extensive data has been archived by Fontes $et\ al$ at NIST:
`http://nlte.nist.gov/OPAC/about.html`

If line-binned opacities are provided as well by data producers then detailed comparison (as opposed to Planck mean) between the opacity data generated by various groups is more easily compared, with respect to the different atomic codes used and the calculations carried-out.

The drawback is for $\tau_l \ll 1$ to hold. Fontes $et\ al$ discuss this at length.

Partition Functions

The (lower) level number density N_l appearing in the optical depth (2) can be written in terms of the ground level number density N_0 (Boltzmann)

$$\frac{N_l}{N_0} = \frac{g_l}{g_0} \mathrm{e}^{-(E_l - E_0)/kT} \tag{4}$$

and the statistical weights g_l and level energies E_l.

The total number density (for any ionization stage) is just

$$N = \sum_l N_l = \frac{N_0}{g_0} U(T) \tag{5}$$

where

$$U(T) = \sum_l g_l \mathrm{e}^{-(E_l - E_0)/kT} \tag{6}$$

is the internal partition function.

Then we can write the level number density as

$$N_l = g_l \mathrm{e}^{-(E_l - E_0)/kT} \frac{N}{U} \,. \tag{7}$$

We note that the summation to determine the partition function in Eq.(6) is *formally divergent.*

In high temperature plasmas (e.g. solar interior) we must introduce occupation factors w_l:

$$U(T) = \sum_l w_l g_l \mathrm{e}^{-(E_l - E_0)/kT} \,. \tag{8}$$

For low-lying levels $w_l \approx 1$ while for high-lying levels $w_l \longrightarrow 0$ due to the surrounding plasma neutralizing the ions at a finite radius. High-lying levels are then part of the continuum (pressure ionization, continuum lowering etc.)

It has been suggested (Carvajal Gallego $et\ al$ 2023) that some works modelling kilonovae have only included the ground level in the partition function, on the grounds that the excited-state populations are small at the low-T under consideration. However, it appears that the weight of the ground configuration was used (Tanaka, this Workshop).
Rule-of-thumb: if a (lower) level contributes to absorption then it contributes to the partition function.

Data Management

Some keywords regarding atomic data:

- Curation
- Provenance
- Reproducibility

NLTE

- Fractional abundances need ionization and recombination rate coefficients
  - Lotz formula for Maxwellian electron-impact ionization **?**
  - Photoionization **?**
  - β-decay **?**
  - Kramers formula for radiative recombination (RR)
  - Burgess formula for dielectronic recombination (DR) not valid here
- Level population determination needs electron-impact excitation rate coefficients and associated radiative rates
  - e.g. DW (AS, HULLAC etc), Dirac R-matrix for EIE

Dielectronic Recombination

Burgess (1964): consider the dielectronic capture process

$$X^{(z+1)+}(i) + \mathrm{e}^- \rightleftharpoons X^{z+}(j, nl) \tag{9}$$

and the possibility that the doubly-excited state (j, nl) radiates rather than autoionizes:

$$X^{z+}(j, nl) \rightarrow X^{z+}(f, nl) + \gamma\,. \tag{10}$$

If the state (f, nl) now lies *below* the ionization limit then we have a stable recombination, and the singly-excited state radiatively cascades its way down to the ground state of X^{z+}. This two-step process is known as *dielectronic recombination*, or DR for short.

Energy conservation gives:

$$k^2 + E(i) = E(j, nl) \approx E(j) - \frac{z^2}{n^2} I_{\mathrm{H}} \qquad (= E(f, nl) + E_\gamma) \tag{11}$$

so that

$$k^2 \approx \Delta E(j - i) - \frac{z^2}{n^2} I_{\mathrm{H}}\,. \tag{12}$$

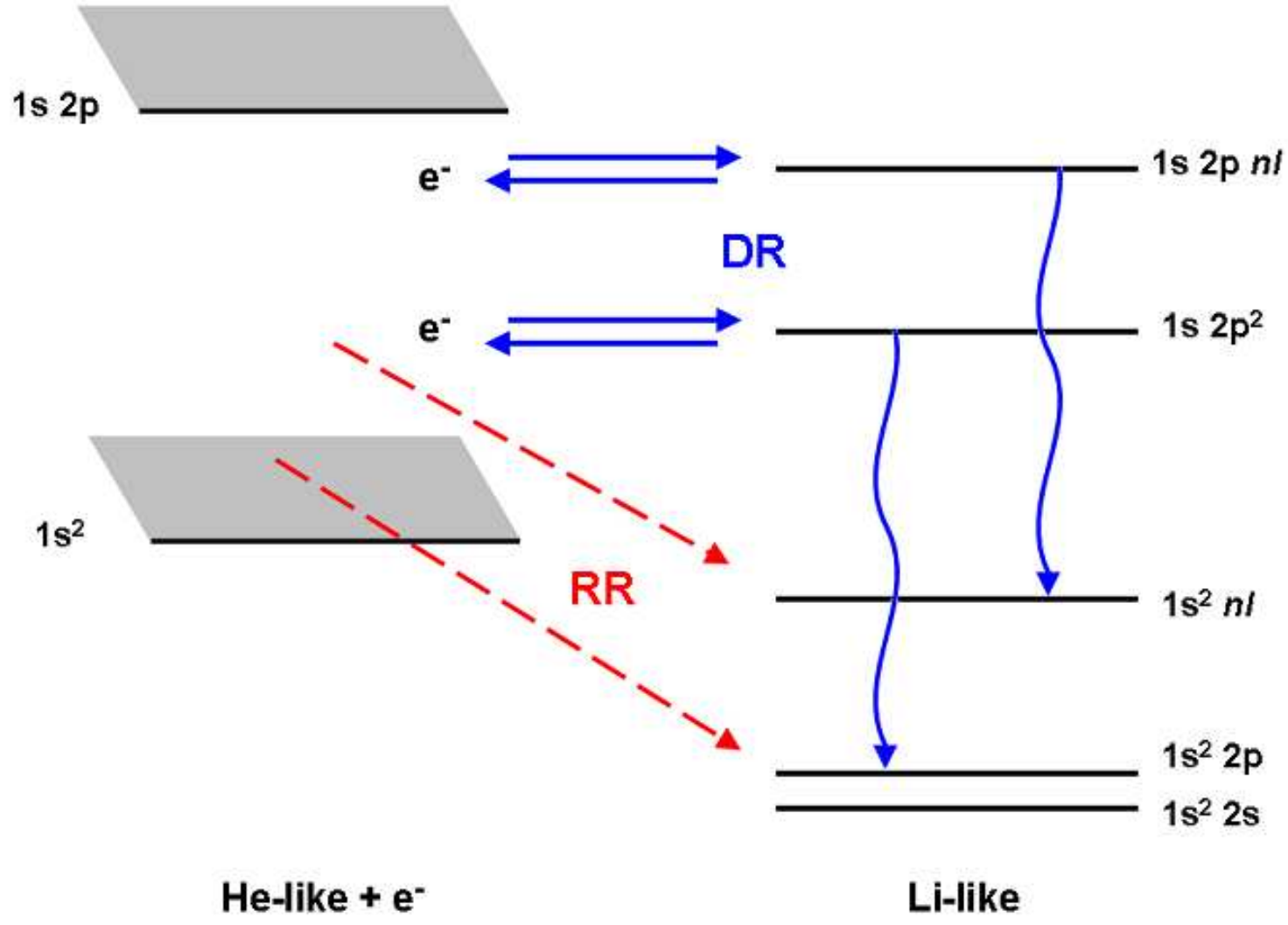

Figure 1: Autoionization, RR and DR.

What is the rate (coefficient) for such a process? It is basically the dielectronic capture rate times the fraction (branching ratio) that radiatively stabilize (with rate $A_{\rm r}$), as oppose to re-autoionize.

Using detailed balance to write the dielectronic capture in terms of its inverse autoionization rate ($A_{\rm a}$), and assuming a Maxwellian distribution (for convenience and plasma applications), the DR rate coefficient is given by

$$\begin{aligned} \alpha_{\rm DR}(i + {\rm e}^- \rightarrow f) &= \left(\frac{4\pi a_0^2 I_{\rm H}}{kT}\right)^{3/2} \sum_j \frac{g_j}{2g_i}\, {\rm e}^{-E/(kT)} \\ &\times \frac{\sum_l A_{\rm a}(j \rightarrow i, kl)\, A_{\rm r}(j \rightarrow f)}{\sum_h A_{\rm r}(j \rightarrow h) + \sum_{m,l} A_{\rm a}(j \rightarrow m, kl)}\,, \end{aligned} \tag{13}$$

where we have summed-over all possible intermediate $(N+1)$-electron resonances, now labelled by j since in general either of the doubly-excited electrons can radiate not just the core one.

Some observations:

Unlike RR, there is no integration over the continuum energy $E = k^2$, since the values are fixed by energy conservation.

The high temperature DR rate coefficient falls-off as $T^{-3/2}$ like the RR.

The low temperature partial DR rate coefficients fall-off exponentially. The amount of 'fill-in' depends on the density of states.

A few resonances just above the ionization limit can give rise to a broad large low temperature contribution because T needs to be very small before the exponential cut-off overwhelms the $T^{-3/2}$.

The total width $(\sum_h + \sum_{ml})$ is the sum over all possible radiative and autoionization pathways out of j.

The $total$ DR rate coefficient is obtained by summing over all final states f which lie below the ionization limit. The reason for this is that, to a good approximation, states which lie above the ionization limit will re-autoionize and so not contribute to net recombination — the Auger cascade can be followed rigorously to test this.

Once excited states ($m > i$) of $X^{z+}(m)$ are energetically accessible then the DR process is highly suppressed.

Consequently, excitation of low-lying states of X^{z+} dominate (but with capture to high-n still) especially those that can radiate via electric dipole transitions.

Since $A_{\rm a} \gg A_{\rm r}$ in general,

$$\frac{A_{\rm a} A_{\rm r}}{A_{\rm a} + A_{\rm r}} \approx A_{\rm r} \tag{14}$$

on dividing top and bottom by $A_{\rm a}$.

Thus, DR is proportional to the $weaker$ of the two depopulating process.

Radiative rates for the core (reverting to $j, nl \longrightarrow f, nl$) are independent of n — the Rydberg electron is simply a spectator.

Autoionization rates scale as n^{-3} since they actively involve the Rydberg electron.

Consequently, the sum over doubly-excited states $j/j, nl$ is a sum over core radiative rates, which is only converged when n gets sufficiently large to attain $A_{\rm a} < A_{\rm r}$ finally, which may not be until $n \approx 1000$.

The statistical weight g_j indicates that this summation can get very large, the l contributions can be to ≈ 15.

Consequently, DR is the dominant electron–ion recombination process in most laboratory and astrophysical non-LTE plasmas.

Because the process often involves high Rydberg states, it is sensitive to density effects — further redistributive collisions before it can radiatively cascade back down to the ground state.

Density effects are not too important in many astrophysical plasmas but are paramount in magnetic fusion plasmas, for example.

Let's look at an example of relevance to kilonovae.

We use AUTOSTRUCTURE (AS) for all calculations — see Badnell (2011) and `http://amdpp.phys.strath.ac.uk/autos/`

A Case Study: DR of Te^{2+}

Tellurium (Te) is used as a representative element in a mixture (along with Ce, Pt & Th) to model late-phase neutron rich ejecta (Pognan *et al* 2022) and Te III emission is seen in AT 2017gfo (Hotokezaka *et al* 2023).

Our starting point to describe DR is the ground configuration of the Sn-like Te^{2+} target [Pd] $5s^2 5p^2$ which has a ${}^3P_{J=0}$ ground term/level.

This is a rather different case to the 4f-shell problem — see e.g. Badnell *et al* (2012) for W XXI $4f^8$ and Hotokezaka *et al* (2021) for Nd III $4f^4$.

We consider the lowest few (N-electron) target configurations:

$5s^2 5p^2$

$5s^1 5p^3$

$5s^2 5p^1 5d^1$

$5s^2 5p^1 4f^1$

$5p^4$ (for mixing with the ground state)

To these user-supplied 5 target configurations, AS will couple a Rydberg nl electron and a corresponding continuum electron (with $l' = l, l \pm 1, l \pm 2 \ldots$).

An example DR reaction pathway then would be:

$$5\mathrm{s}^2 5\mathrm{p}^2 + \mathrm{e}^- \rightleftharpoons 5\mathrm{s}^2 5\mathrm{p} 5\mathrm{d} nl \rightarrow 5\mathrm{s}^2 5\mathrm{p}^2 nl + \gamma \, .$$

AS automatically loops over $n = 6 - 1000$ and $l = 0 - 8$ (in this case) treating each nl separately — no Rydberg n- or l-mixing — calculating all possible autoionization & radiative rates and energies.

Full configuration mixing is maintained between the N-electron target/core $for\ all\ nl$, i.e. Hamiltonians are always diagonalized and no rates are determined by extrapolation. (Similarly for the $(N+1)$ recombined ones.)

We need to consider also outer electron radiation. AS considers two cases:

1/ $nl \rightarrow 5l'$, i.e. into the core.

2/ $nl \rightarrow n'l'$, for $n > 5$, i.e. Rydberg-Rydberg, and which is treated hydrogenically.

So, to represent $1/$, the user-supplied 5 target configurations are supplemented by $(N+1)$-electron configurations formed by adding any of our $5\mathrm{s}, 5\mathrm{p}, 5\mathrm{d}, 4\mathrm{f}$ orbitals to any/all of the 5 N-electron ones. These can be generated automatically by AS, or user supplied if 'awkward' ones are internally generated.

There are twelve here:

$5\mathrm{s}^2 5\mathrm{p}^3 5\mathrm{d}^0 4\mathrm{f}^0$, $5\mathrm{s}^2 5\mathrm{p}^2 5\mathrm{d}^1 4\mathrm{f}^0$, $5\mathrm{s}^2 5\mathrm{p}^2 5\mathrm{d}^0 4\mathrm{f}^1$, $5\mathrm{s}^1 5\mathrm{p}^4 5\mathrm{d}^0 4\mathrm{f}^0$,
$5\mathrm{s}^1 5\mathrm{p}^3 5\mathrm{d}^1 4\mathrm{f}^0$, $5\mathrm{s}^1 5\mathrm{p}^3 5\mathrm{d}^0 4\mathrm{f}^1$, $5\mathrm{s}^2 5\mathrm{p}^1 5\mathrm{d}^2 4\mathrm{f}^0$, $5\mathrm{s}^2 5\mathrm{p}^1 5\mathrm{d}^1 4\mathrm{f}^1$,
$5\mathrm{s}^2 5\mathrm{p}^1 5\mathrm{d}^0 4\mathrm{f}^2$, $5\mathrm{s}^0 5\mathrm{p}^5 5\mathrm{d}^0 4\mathrm{f}^0$, $5\mathrm{s}^0 5\mathrm{p}^4 5\mathrm{d}^1 4\mathrm{f}^0$, $5\mathrm{s}^0 5\mathrm{p}^4 5\mathrm{d}^0 4\mathrm{f}^1$.

An example DR reaction pathway here would be:

$$5\mathrm{s}^2 5\mathrm{p}^2 + \mathrm{e}^- \rightleftharpoons 5\mathrm{s}^2 5\mathrm{p} 5\mathrm{d} nl \rightarrow 5\mathrm{s}^2 5\mathrm{p}^2 5\mathrm{d} + \gamma$$

for $l = 0, 2$.

These 12 $(N+1)$-electron configurations also describe the case of dielectronic capture into $n = 5$, followed by radiative stabilization amongst them.

2/ A relevant example DR reaction pathway involving Rydberg-Rydberg radiative stabilization is (the $5\mathrm{s}^2$ has been suppressed here):

$$5\mathrm{p}^{2\,3}\mathrm{P}_{J=0} + \mathrm{e}^- \rightleftharpoons 5\mathrm{p}^{2\,3}\mathrm{P}_{J=1,2}\, nl \rightarrow 5\mathrm{p}^{2\,3}\mathrm{P}_{J=1,2}\, n'l' + \gamma$$

We can rewite the Rydberg energy conservation formula Eq.(12) with $k^2 = 0$ to estimate the n-value at which this pathway becomes energetically allowed:

$$n \approx z/\sqrt{\Delta E(j-i)}\,. \tag{15}$$

Using the observed (preferably) splittings (in Rydbergs)

$J = 0$ 0.0
$J = 1$ 0.04329
$J = 2$ 0.07440

with $z = 2$, we obtain $n = 10$ (on rounding up) for $J = 0 \rightarrow 1$ and $n = 8$ for $J = 0 \rightarrow 2$, at which dielectronic capture is energetically allowed.

Correspondingly, suppression of DR via $J = 0 \rightarrow 2$ capture by $J = 2 \rightarrow 1$ autoionization opens-up at $n = 12$.

So, we see that excitation of the lowest level should give the largest contribution to DR at low-T. And, equally, DR from the first excited $J = 1$ initial level opens-up at $n = 12$, but is already suppressed by autoionization back to the ground level.

More generally, the lowest 5 levels in Te^{2+} are not connected to lower levels by electric dipole radiation. Thus, population may build-up in them.

Thus, we consider DR from the 5 lowest initial levels of the ground configuration: $^3\mathrm{P}_{J=0,1,2}$, $^1\mathrm{D}_{J=2}$ and $^1\mathrm{S}_{J=0}$.

Time for some figures!

Before we look at Maxwellian rate coefficients, it is a of interest to convolute the underlying binned(!) DR cross sections with a typical experimental distribution.

The CRYRING heavy-ion storage ring has recently been reborn at GSI Darmstadt. (In an earlier life in Stockholm it measured DR of light ions.) One of its programs is to consider the DR of low-charge heavy ions such as Xe. This can likely benchmark DR data for kilonovae.

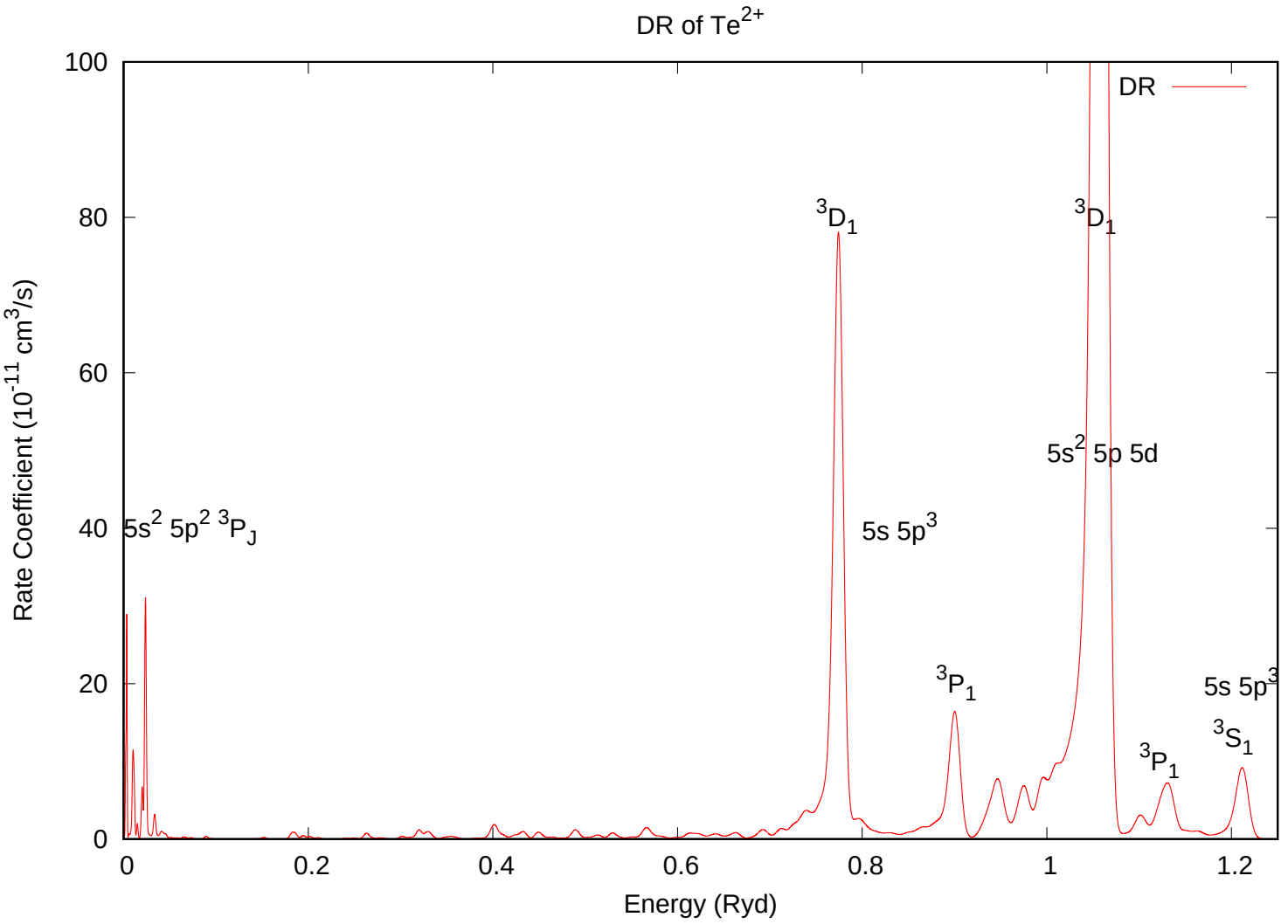
DR of Te2+
DR
Rate Coefficient (10-11 cm3/s)
Energy (Ryd)
0
20
40
60
80
100
0
0.2
0.4
0.6
0.8
1
1.2
5s2 5p2 3PJ
3D1
5s 5p3
3P1
5s2 5p 5d
3D1
3P1
5s 5p3
3S1

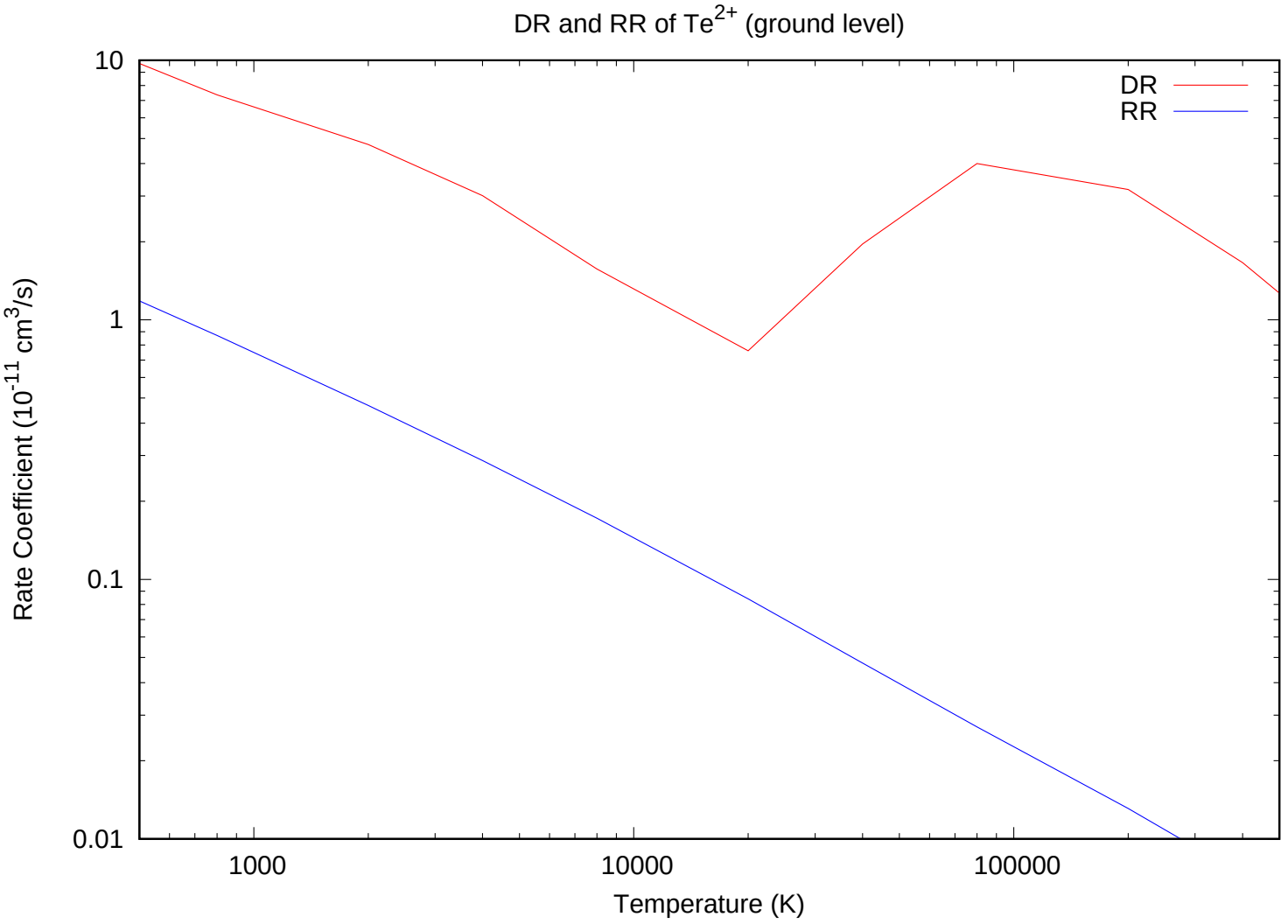
DR and RR of Te2+ (ground level)
DR
RR
Rate Coefficient (10-11 cm3/s)
10
1
0.1
0.01
1000
10000
100000
Temperature (K)

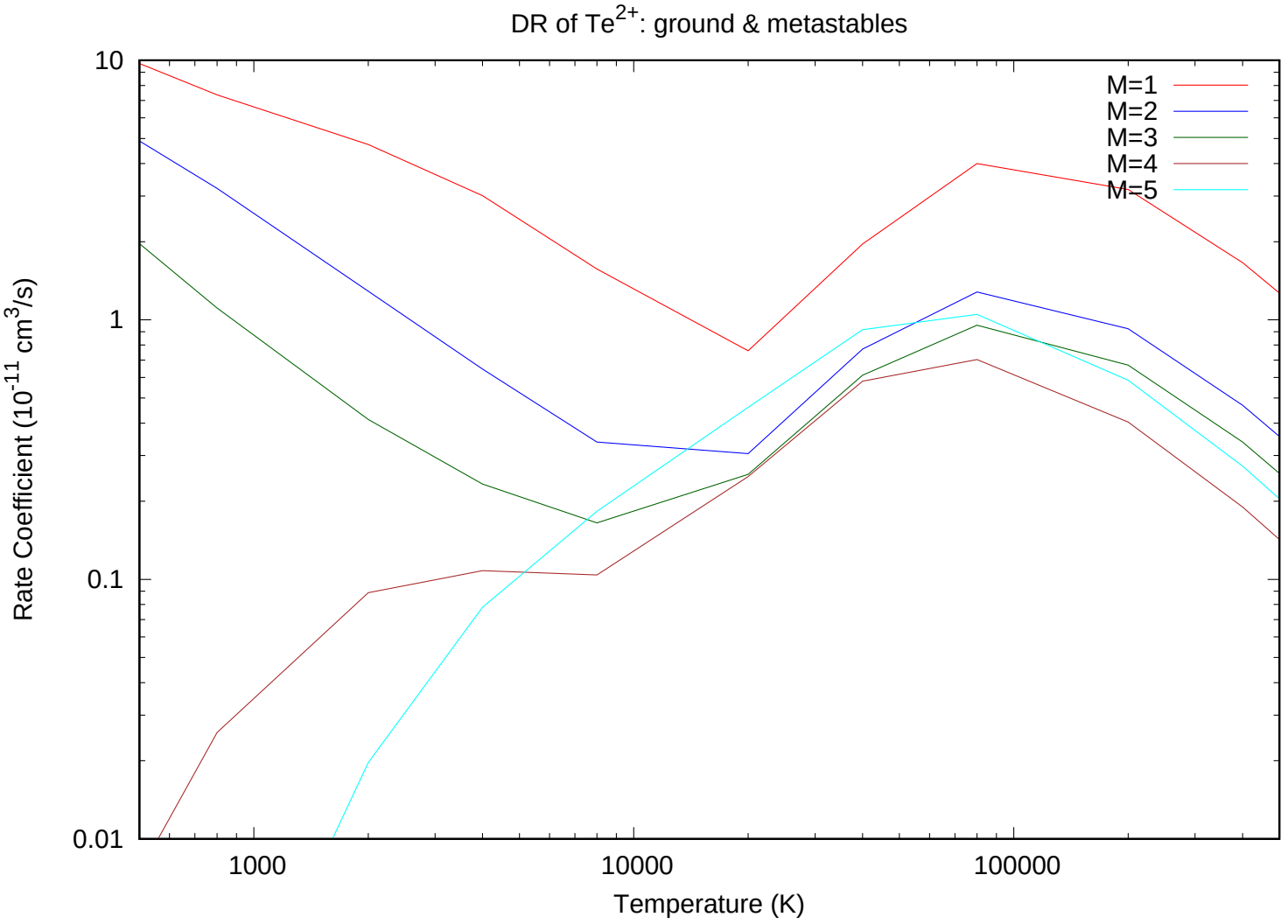
DR of Te2+: ground & metastables
Rate Coefficient (10-11 cm3/s)
Temperature (K)
10
1
0.1
0.01
1000
10000
100000
M=1
M=2
M=3
M=4
M=5

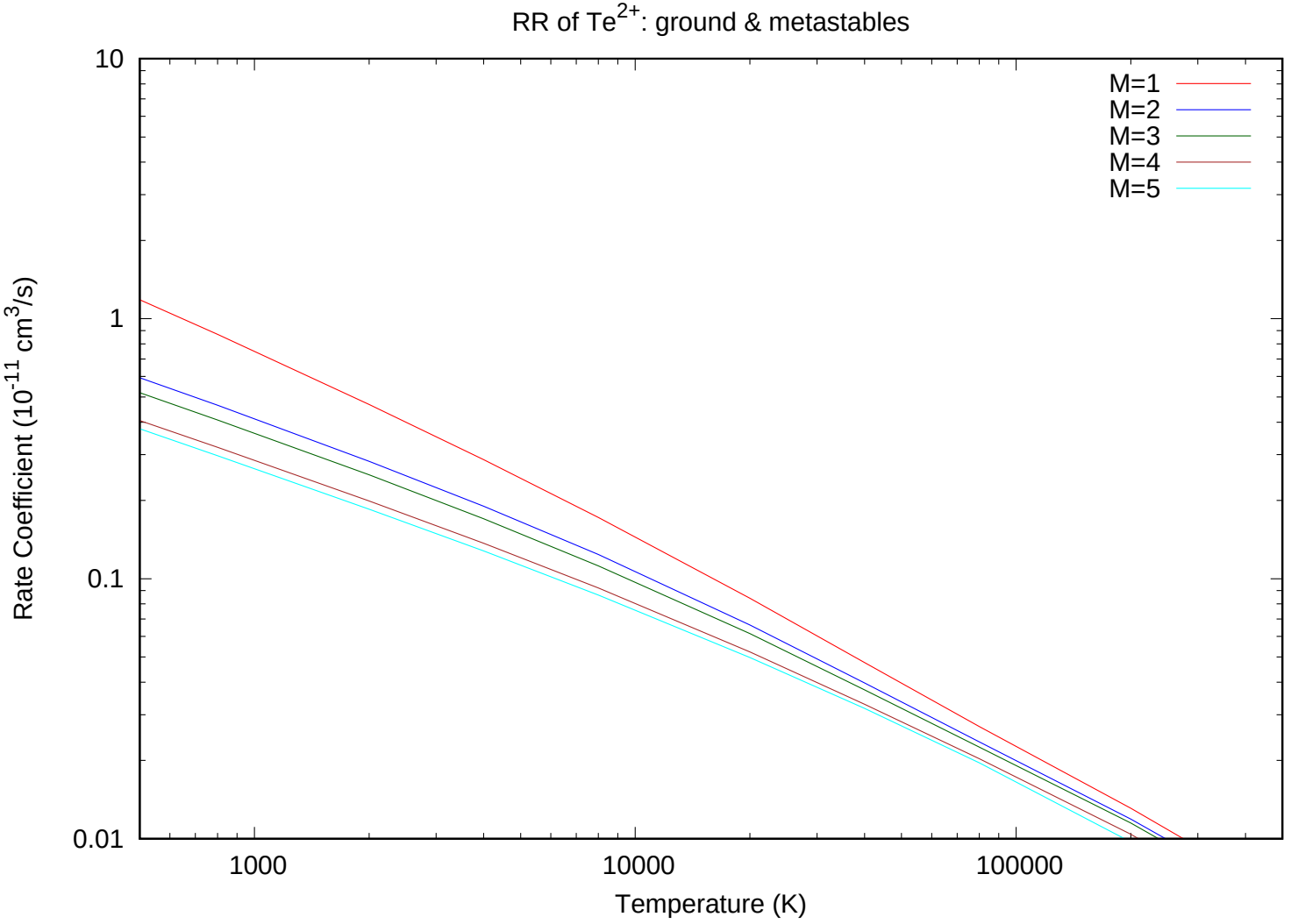
RR of Te2+: ground & metastables
Rate Coefficient (10-11 cm3/s)
Temperature (K)
10
1
0.1
0.01
1000
10000
100000
M=1
M=2
M=3
M=4
M=5

AS code availability

The current Gold version of AS (v29.x) is publically available at:

`http://amdpp.phys.strath.ac.uk/autos`

There are detailed online instructions on how to install the code
(basically, at the command line type: gfortran asdeck29.f95 -o aslm29.x)

and how to run it
(basically, at the command line type: ./aslm29.x <das)
using of the many example datasets (das) provided there to play with.

Every year, several final year B.Sc. and M.Sci. students embark on research projects involving AS. They are directed to this web page and its notes and told to get on with it!

Key Points for Kilonovae

LTE: Latest opacities look to be converging to better than a factor of 2.

NLTE: DR likely dominates RR for any ion with fine-structure levels within the ground term, not just complex species such as $4f^n$.

Acknowledgements

The work of the UK APAP Network is supported by the UK STFC under Grant No. ST/V000683/1 with the University of Strathclyde.

References (selected)

Badnell N. R., Comp. Phys. Commun. 182, 1528 (2011)
Badnell N. R., *et al* Phys.Rev. A85, 052716 (2012)
Banerjee S. *et al* , ApJ 934, 117 (2022)
Bar-Shalom A.*et al* , JQSRT 71, 169 (2001)
Burgess A, ApJ 139, 776 (1964)
Carvajal Gallego H. *et al* , MNRAS 518, 332 (2023)
Carvajal Gallego H. *et al* , MNRAS 522, 312 (2023)
Carvajal Gallego H. *et al* , EPJD 77, 72 (2023)
Cowan R. D. *The Theory of Atomic Structure and Spectra* University of California Press, Berkeley, CA (1981)
Even W. *et al* , ApJ 899, 24 (2020)
Fontes C. J. *et al* , MNRAS 493, 4143 (2020)
Fontes C. J. *et al* , MNRAS 519, 2862 (2023)
Gu M. F., Can.J.Phys. 68, 675 (2008)
Hotokezaka K. *et al* , MNRAS 506, 5863 (2021); At Press (2023)
Kasen D.*et al* , ApJ 774, 25 (2013)
Kasen D.*et al* , Nature 551, 2 (2017)
Pognan Q. *et al* , MNRAS 513, 5174 (2022)
Sampson D. H. *et al* , Phys.Rep. 477, 111 (2009)
Tanaka M. *et al* , MNRAS 496, 1369 (2020)